

Structural, electronic and magnetic properties of partially inverse spinel CoFe_2O_4 : a first-principles study

Y H Hou¹, Y J Zhao², Z W Liu¹, H Y Yu¹, X C Zhong¹, W Q Qiu¹,
D C Zeng¹ and L S Wen¹

¹ School of Materials Science and Engineering, South China University of Technology, Guangzhou, 510640, People's Republic of China

² Department of Physics, South China University of Technology, Guangzhou, 510640, People's Republic of China

E-mail: medczeng@scut.edu.cn

Received 14 June 2010, in final form 13 September 2010

Published 21 October 2010

Online at stacks.iop.org/JPhysD/43/445003

Abstract

Partially inverse spinel CoFe_2O_4 , which may be prepared through various heat treatments, differs remarkably from the ideal inverse spinel in many properties. The structure of partially inverse spinel CoFe_2O_4 as well as its electronic and magnetic properties through a systemic theoretical calculation of $(\text{Co}_{1-x}\text{Fe}_x)_{\text{Tet}}(\text{Co}_x\text{Fe}_{2-x})_{\text{Oct}}\text{O}_4$ ($x = 0, 0.25, 0.5, 0.75$ and 1.0) have been investigated by the generalized gradient approximation (GGA) + U approach. It is found that the Co and Fe ions prefer their high spin configurations with higher spin moments at octahedral sites in all the studied cases, in line with experimental observations. The Co ions at the octahedral sites favour being far away from each other in the partial inverse spinels, which also show half metallicity at certain inversion degrees.

(Some figures in this article are in colour only in the electronic version)

1. Introduction

The spinel AB_2X_4 is one of the most interesting and important families of crystalline compounds, with applications in magnetic materials, ceramics, catalysis, etc [1]. A , B and X denote a divalent cation, a trivalent cation and a divalent anion, respectively, in the stoichiometric formula of AB_2X_4 , including oxides, sulfides, selenides and tellurides [2–4]. Spinel ferrites [5] have been studied for many years due to their performance in high-frequency devices. In particular, the spinel cobalt ferrite (CoFe_2O_4) has covered a wide range of applications including electronic devices, ferrofluids, magnetic delivery microwave devices and high density information storage due to its wealth of magnetic and electronic properties, such as high magnetostriction and high rate of change of strain with magnetic field, cubic magnetocrystalline anisotropy, high coercivity, moderate saturation magnetization, high Curie temperature T_C , photomagnetism, high chemical stability and good electrical insulation [6–18].

The cations A and B can occupy two different sites in a spinel structure, i.e. octahedral (O_h) and tetrahedral (T_d)

sites within the fcc oxygen sublattices. The occupations of metals at O_h and T_d sites have an important effect on the properties of spinels, such as colour, diffusivity, magnetic behaviour, conductivity and catalytic activity [19–21]. The actual distribution of cations A and B in spinels is influenced by the heat treatment process and chemical environment [22]. The cation distribution can be distinctly characterized by the so-called degree of inversion x , which is defined as the fraction of the divalent metal cations in octahedral sites as follows:



In normal spinels ($x = 0$), the tetrahedral and octahedral sites are occupied by divalent and trivalent cations, respectively, while in the inverse spinels ($x = 1$) all the divalent cations occupy the octahedral sites and trivalent cations occupy tetrahedral and octahedral sites evenly. When it is a partial inverse structure, the spinel is called disordered since the di- and trivalent cations may be distributed at both tetrahedral and octahedral sites. The numbers of trivalent and divalent ions are required to remain at 2:1 in a stable AB_2X_4 . Typical

normal spinels at room temperature are MgAl_2O_4 , FeAl_2O_4 , ZnAl_2O_4 and FeCr_2O_4 , while Fe_3O_4 , MgFe_2O_4 and NiFe_2O_4 are typical inverse spinels [23]. The structure of spinel oxides can accommodate various cations, some of which may have multiple oxidation states, distributing at the tetrahedral and octahedral sites in different ways. For instance, Co ions of both 2+ and 3+ oxidation state can co-exist in the Co_2FeO_4 ferrites, and so do Fe ions in the Fe_3O_4 ferrites. Determination of the cation distribution is a crucial issue since it plays an important role in the properties of spinels [24].

Many researchers have reported that the actual cation distribution of cobalt ferrite depends on heat treatments [24–30]. Part of the Co^{2+} may be located at the octahedral sites under different heat treatment processes, and a range 0.62–0.93 for the inverse parameter x is reported. Mössbauer spectroscopy measurements have suggested $x \approx 0.76$ when samples annealed at 1520 K if they are water quenched, and $x \approx 0.93$ if slowly cooled [25, 26]. Meanwhile, $x \approx 0.62$ was measured when the samples annealed at 1320 K and quenched in water [27, 28], and $x \approx 0.80$ was reported for CoFe_2O_4 prepared at 870 K [29]. A synchrotron x-ray diffraction study, making use of anomalous x-ray scattering, suggested $x \approx 0.78$ when a sample annealed at 1073 K, though no details were given about the cooling conditions [30]. Analysis of the powder XRD data of CoFe_2O_4 samples annealed at 1170 K suggested $x \approx 0.75$ [24].

Theoretical studies [8, 31–34] have focused on ideal inverse and normal spinels of CoFe_2O_4 by the local spin density approximation (LSDA) [8, 31] and beyond, for example, by invoking the on-site Coulomb repulsion energy (U) through the LSDA + U [32] and GGA + U (generalized gradient approximation + U) approaches [33] or using the self-interaction corrected (SIC)-LSDA method [34]. The LSDA approach usually describes these materials to be half-metallic or metallic, if no distortions are included. The transition metal (TM) d electrons in oxides (as well as f electrons in rare earth compounds) are generally strongly correlated and cannot be adequately described within the standard band theory framework with such approximations as LSDA or GGA, which place them too close to the Fermi level. The LDA + U or GGA + U approach, treating the Hubbard U as an adjustable parameter, has correctly described CoFe_2O_4 as insulators. The SIC-LSDA method, which is parameter free, may provide a better description of correlations than LSDA, but requires a much heavier computing resources than LDA + U or GGA + U .

In this paper we mainly apply the GGA + U approximation to study the optimal electronic structure of CoFe_2O_4 at different degrees of inversion. The electronic and magnetic properties of these systems were investigated by systematically varying cation distributions ($x = 0.0, 0.25, 0.50, 0.75$ and 1.0). This contributes to the understanding of the global behaviour exhibited by the known (observed) and new (expected) $(\text{Co}_{1-x}\text{Fe}_x)_{\text{Tet}}[\text{Co}_x\text{Fe}_{2-x}]_{\text{Oct}}\text{O}_4$ spinels in terms of local and microscopic properties. Our results show that the Co ions strongly prefer the octahedral sites, and the temperature effect-induced tetrahedral site Co ions like to be far away from the octahedral site Co. It also indicates that the Co and Fe ions always prefer the high spin configurations in the studied normal, inverse and partial inverse spinel CoFe_2O_4 .

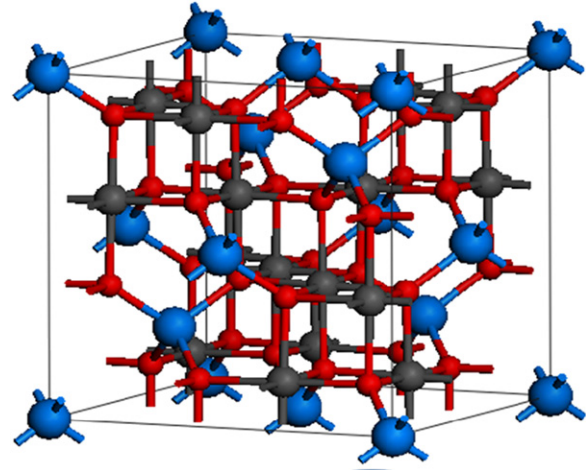


Figure 1. The cubic cell of spinel structure. The tetrahedral and octahedral cation sites are denoted by blue and dark gray spheres, respectively, while the oxygen atoms are represented by the small red spheres.

2. Computational details

2.1. Crystal modelling

The conventional unit cell of the spinel structure contains eight formula units as shown in figure 1, and it belongs to the $Fd\bar{3}m$ space group (227). Cations occupy 8a and 16d special Wyckoff positions of T_d and O_h symmetries at $(0, 0, 0)$ and $(5/8, 5/8, 5/8)$, respectively, whereas oxygen ions occupy the 32e positions at (u, u, u) [35]. Here u is the positional parameter of oxygen. It should be noted that the spinel is a relatively open structure since cations only occupy around 33% volume of the octahedral and tetrahedral voids [36].

According to various occupations of Co and Fe ions, we calculated two types of structures for $x = 0.25$, three types of structures for both $x = 0.5$ and $x = 0.75$ considered in a 28-atom cell, and one type of structure for $x = 0$ and 1 in a 14-atom cell. For the convenience of description, different structures with the same x are denoted by their symmetry. For example, when the Co ion at the fractional coordinates $(1, 1, 1)$ in a cubic cell of the normal spinel structure exchanges with the Fe ion at $(5/8, 7/8, 7/8)$, the symmetry reduces to CM , and thus we identify this structure as $0.25(CM)$. Analogous notations are adopted for other structures.

2.2. Computational method

We performed the electronic structure calculation and structure optimization through the Vienna *Ab initio* Simulation Package (VASP) [37, 38], with Perdew–Burke–Ernzerhof parametrized GGA [39] and the projector augmented-wave (PAW) method [40, 41]. The plane-wave expansion was truncated at a cutoff energy of 450 eV in all of our calculations. The optimizations were performed with a $3 \times 3 \times 3$ k-mesh for the partial inverse structure unit cells consisting of 28 atoms and with a $7 \times 7 \times 7$ k-meshes for the normal and inverse structure unit cells consisting of 14 atoms. The relaxations of lattices are stopped until the forces on each ion are converged to

less than $1 \text{ meV } \text{\AA}^{-1}$. For the final total energy calculations, the tetrahedron method of a $7 \times 7 \times 7$ k-mesh for the 28-atom cell and a $9 \times 9 \times 9$ k-mesh for the 14-atom cell are used. The convergence was tested for $x = 1$ and $x = 0.75$ cases, which indicates that the total energy changes within 1 meV when the k-mesh is increased from $7 \times 7 \times 7$ to $9 \times 9 \times 9$ for a 28-atom cell, and within 10 meV/formula when the energy cutoff is increased from 450 to 550 eV. In both the structure optimization and electronic structure calculation, the Néel configuration is chosen as the initial magnetic configuration, where the magnetic moments on tetrahedral and octahedral sites are antiparallel to each other.

The density functional theory GGA + U methodology [42–44] has been employed for the final calculations on total energy, electronic structure and magnetic properties. Here we use the simple formulation by Liechtenstein *et al* [42] and Dudarev *et al* [43], where a single parameter U_{eff} determines the orbital-dependent correction to the DFT energy. U_{eff} is generally expressed as the difference between parameters U and J . The Hubbard U is the Coulomb-energetic cost to place two electrons at the same site, and J is an approximation to the Stoner exchange parameter. For the inverse cobalt ferrite, a series of calculations with U_{eff} varying from 2 to 6 eV for Fe and Co 3d orbital have been conducted. It is found that the total magnetic moment and local moment for the cations change within $0.04 \mu_{\text{B}}$ /formula and $0.28 \mu_{\text{B}}$ /cation, respectively. Meanwhile, the value of the energy gap strongly depends on the choice of U_{eff} . In order to be consistent with experimental reported magnetic moments and theoretical gap values in the earlier literature, we finally employed $U = 4.22 \text{ eV}$ (as in [44]) and $J = 0.80 \text{ eV}$ for Fe, and $U = 4.08 \text{ eV}$ (as in [44]) and $J = 0.79 \text{ eV}$ for Co in this work.

3. Results and discussion

3.1. Energetics of CoFe_2O_4

The calculated energies of various CoFe_2O_4 configurations relative to its ideal inversion spinel are listed in table 1, and illustrated in figure 2. It shows that the most stable structure is the inverse spinel structure with all the Co ions located at the octahedral sites, while the normal spinel structure is the most unstable. The total energy of CoFe_2O_4 increases as the inversion degree decreases.

For $x = 0.25$, Co ions can be located at the octahedral site at $(0.0625, 0.0625, 0.5625)$ or $(0.3125, 0.3125, 0.3125)$, and denoted for CM and $R3M$, respectively, in a 28-atom cell. It is found that the CM configuration is more stable than $R3M$ by 0.1 eV/Co , indicating that Co (O_h) prefers to be far away from Co (T_d).

For $x = 0.50$, we considered three structures, namely $C2M$, CM and $P-1$. It is found that the $C2M$ configuration with Co ions located at $(0.0625, 0.0625, 0.5625)$ and $(0.5625, 0.0625, 0.0625)$ is energetically favoured. It also shows the two Co (O_h) atoms favour being far away from each other and also far away from Co (T_d) relatively.

For $x = 0.75$, we considered three structures, CM , $P1$ and $R3M$. It is found that the configuration with space group of CM

Table 1. Theoretical and experimental lattice parameters and the relative energies of bulk $(\text{Co}_{1-x}\text{Fe}_x)_{\text{Tet}}(\text{Co}_x\text{Fe}_{2-x})_{\text{Oct}}\text{O}_4$ for different values of the inversion parameter x . Here u stands for the internal coordinate of a represented oxygen atom.

x	u	$A(\text{\AA})$	$\Delta E \text{ (eV/Co)}$
<i>Theoretical</i>			
0.0	0.380	8.308	0.339(0.20 ^a)
0.25($R3M$)	0.380	8.325	0.382
0.25(CM)	0.381	8.334	0.281
0.50($P-1$)	0.379	8.338	0.255
0.50(CM)	0.381	8.336	0.223
0.50($C2M$)	0.381	8.337	0.205
0.75($R3M$)	0.375	8.343	0.201
0.75($P1$)	0.379	8.340	0.190
0.75(CM)	0.379	8.355	0.113
1.0	0.378	8.384(8.400 ^a , 8.379 ^b)	0
<i>Experimental</i>			
0.75	0.381 ^c	8.381 ^c , 8.294 ^d	
1.0	0.380 ^e	8.390 ^e	

Note: ΔE is relative to the total energy of the inverse spinel.

^a from [33].

^b from [34].

^c from [24].

^d from [45].

^e from [35].

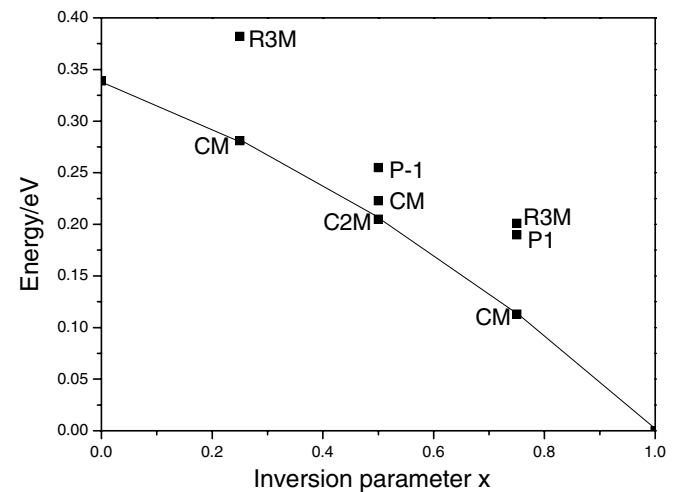


Figure 2. Calculated energies (eV/Co) relative to the total energy of the inverse spinel for $(\text{Co}_{1-x}\text{Fe}_x)_{\text{Tet}}(\text{Co}_x\text{Fe}_{2-x})_{\text{Oct}}\text{O}_4$ spinels with $x = 0, 0.25, 0.50, 0.75$ and 1.0 .

with Co ions located at the $(0.0625, 0.5625, 0.5625)$, $(0.5625, 0.0625, 0.0625)$ and $(0.3125, 0.3125, 0.3125)$ is preferred energetically. It also indicates that Co (O_h) prefer to be away from each other in the octahedral surrounding. Therefore, Co ions will be distributed rather uniformly in the experimentally prepared partially inverted samples. This also indicates that the relatively small unit cells adopted in this work for various inverse spinels are reasonable.

The site preference of Co and Fe ions at the spinel structure is determined by their corresponding Gibbs free energies, which are dominated by their size effect, Coulomb interaction with oxygen lattice, as well as the temperature dependent entropy contribution. In CoFe_2O_4 , there are six surrounding oxygen ions at the octahedral site, which will have a stronger Coulomb attraction with Fe^{3+} ions than the tetrahedral site

Table 2. Calculated magnetic moments (μ_B) for Co, Fe, and total for one formula unit of $(\text{Co}_{1-x}\text{Fe}_x)_{\text{Tet}}(\text{Co}_x\text{Fe}_{2-x})_{\text{Oct}}\text{O}_4$ as well as the band gaps for various x . Positive and negative values represent majority spin and minority spin, respectively.

X	Co ^{tet}	Co ^{oct}	Fe ^{tet}	Fe ^{oct}	M_{total}	Band gap (eV)
<i>Theoretical</i>						
0.0	-2.42 (-2.45 ^a , -2.58 ^b)			4.12 (4.06 ^a , 4.13 ^b)	7	0.09
0.25(CM)	-2.44	2.67	-3.96	4.13	6	0.08
0.25(R3M)	-2.44	2.75	-3.97	4.12	6	0.00
0.50(C2M)	-2.45	2.63	-3.95	4.12	5	0.16
0.50(CM)	-2.44	2.64	-3.96	4.12	5	0.24
0.50(P-1)	-2.43	2.64	-3.95	4.12	5	0.00
0.75(CM)	-2.43	2.62	-3.97	4.11	4	0.30
0.75(P1)	-2.41	2.63	-3.96	4.10	4	0.00
0.75(R3M)	-2.42	2.62	-3.95	4.10	4	0.00
1.0		2.61 (0.13 ^a , 2.58 ^b , 2.58 ^c)	-3.97 (-3.51 ^a , -4.11 ^b , -3.93 ^c)	4.10 (4.05 ^a , 4.10 ^b , 4.08 ^c)	3 (3 ^b , 3 ^c)	0.72 (0.52 ^a , 0.80 ^b , 0.63 ^c , 0.60 ^d)
<i>Experimental</i>						
0.96 ^e					3.4	
0.79 ^e					3.9	
0.69 ^f	-3.08*	3.21*	-3.08*	3.21*		

Note: “*” values are averaged for Co and Fe at corresponding sites in [49].

^a from [33].

^b from [34].

^c from [32].

^d from [48].

^e from [26].

^f from [49].

with four surrounding oxygen ions. Meanwhile, the interstitial octahedral site has a larger space than that of the tetrahedral site, and thus Co^{2+} ions prefer the octahedral site from the size effect aspect since it has a radius of 0.72 Å, which is greater than that of Fe^{3+} ions, 0.64 Å [46]. As a result, the site preference will be a competition between the size effect and Coulomb interaction under low temperature, where the entropy contribution is negligible. Our calculation indicates that the size effect prevails over the Coulomb effect, as the normal spinel structure is energetically higher than that of the ideal inverse spinel by 0.339 eV/Co. As the temperature increases, the entropy contribution has a remarkable influence on the distribution of Co and Fe ions, as the various partial inverse spinel structures reported in experiments. Although we have investigated several partial inverse spinel structures, it is clear that the inversion parameter x depends on the heat treatments since our calculated energy for the configurations increases as x decreases. However, the direct correlation between the heat treatments (mainly temperature) requires Monte Carlo simulation with more energy information for various configurations, which needs great computational effort. It is worth noting that the inverse degree of CoFe_2O_4 will not be smaller than 0.5 at the limit of high temperature, although the structures of $x = 0.25$ and 0 are studied in this work.

The optimized structural parameters are also summarized in table 1, in comparison with available experimental and theoretical data in the literature. The equilibrium structural parameters of CoFe_2O_4 in the inverse spinel configuration ($x = 1$) is found to be $a = 8.384$ Å and $u = 0.378$, which is in excellent agreement with the experimental values of $a = 8.390$ Å and $u = 0.380$. As the inverse parameter x decreases from 1 to 0, the lattice parameter increases slightly

by less than 1%, with little changes for the internal coordinates of oxygen.

The calculated bond lengths of both Co–O and Fe–O at the tetrahedral sites are about 1.86 Å, while those at the octahedral sites are around 2.02 Å. There is no remarkable difference between the bond length of Co–O and Fe–O when they are at the same type of interstitial sites, in line with the negligible lattice change as x changes from 1 to 0. We note that the bond length of Co–O and Fe–O at the tetrahedral sites for the ideal inverse spinel obtained by Walsh *et al* [33] is longer than ours by about 0.1 Å, while those at the octahedral sites are in good agreement. This could result from the incorrect spin configuration obtained in [33] for cations at the tetrahedral sites, which will be discussed in detail in the next section.

3.2. Magnetic properties and electronic structures

The spin configurations of various spinel structures ($x = 0$ to 1) are investigated to illustrate the nature of the magnetic properties of the CoFe_2O_4 spinels. Fe ions and Co ions are possessed of different local symmetries at different lattice sites. According to the crystal field (CF) theory, the e_g levels are lower than the t_{2g} levels in a tetrahedral CF due to the direct electrostatic repulsion between the d_{xy} , d_{yz} and d_{zx} orbitals and surrounding anion orbitals, while the order is reversed in the octahedral environment as the d_{z^2} and $d_{x^2-y^2}$ orbitals are repelled directly. The electronic configuration depends on the relative strength of the CF and intra-atomic exchange field (EF), which results in possible high spin (CF < EF) or low spin (CF > EF) configurations [19].

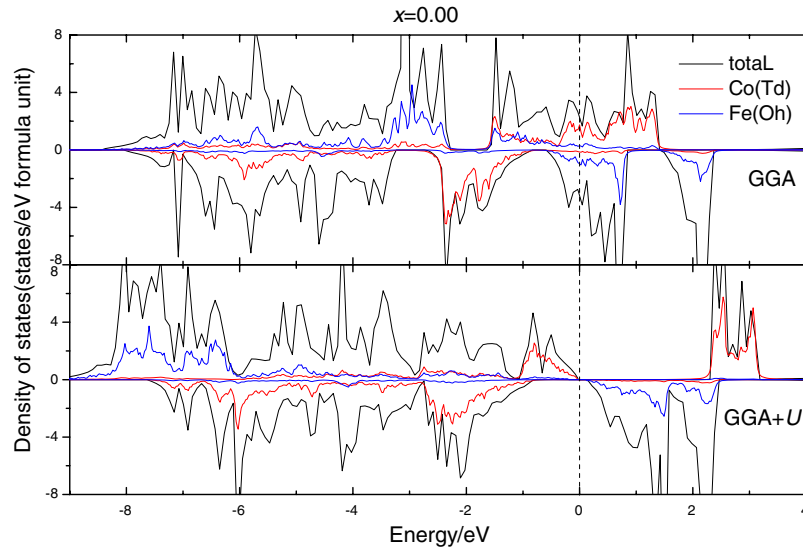


Figure 3. The atom-projected DOS and TDOS of CoFe_2O_4 with the normal spinel structure. The minority DOS is set to negative, while the majority part is set to positive. VBM is set to 0.

The calculated magnetic moments (μ_B) of Co and Fe ions, and their total magnetic moment are listed in table 2 for the considered cases. It shows that the total magnetic moment decreases with increasing x , in line with the experimental observation in [47], which found that the saturation magnetization increases with increasing heat treatment temperature, implying that there is a net exchange of Co ions at octahedral sites with the Fe ions at tetrahedral sites.

The total and projected densities of states (DOS) of normal cobalt ferrite given by GGA and GGA+ U are compared in figure 3. From table 2 and figure 3, it is clear that our calculated results correspond to a typical high spin (relative strong exchange splitting) configuration for both Co and Fe ions at the tetrahedral and octahedral sites, where three and five unpaired electrons are expected per Co^{2+} and Fe^{3+} , respectively, leading to a final magnetic moment of $7\mu_B$ per CoFe_2O_4 formula for the ideal normal spinel structure. The e_g levels of Co ion are completely filled at the tetrahedral sites, while the t_{2g} levels are half filled by the unpaired electrons for Co^{2+} ion.

Meanwhile both the t_{2g} and e_g levels of Fe^{3+} at both tetrahedral and octahedral sites are half occupied by the unpaired electrons, as schematically shown in figure 4. Figure 3 also shows that cobalt ferrite in the normal spinel structure is metallic in GGA calculation and becomes insulating with a small band gap of 0.09 eV when $U = 4.22$ eV and $J = 0.80$ eV for Co and $U = 4.08$ eV and $J = 0.79$ eV for Fe is applied. It is noted here that low spin configuration of Co^{3+} ion at the octahedral site is reported in the theoretical work by Walsh *et al* [33], while our results show that CoFe_2O_4 for $x = 1.0$ favours high spin configuration and the valence of Co at the octahedral site is 2+. To clarify the spin configuration of Co (O_h), we have also studied the case of low spin for Co ion, which indicates that the energy of low spin case is 0.71 eV per Co higher than that of high spin case. On the other hand, the high spin configuration of Co ion in Cobalt ferrite is in agreement with most theoretical and experimental results in the literature [24, 47].

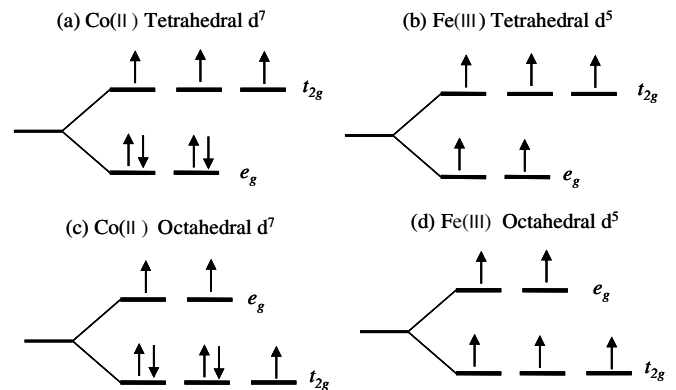


Figure 4. Electronic configuration for the Co^{2+} and Fe^{3+} ions in T_d and O_h coordination in cobalt ferrite. All the tetrahedral and octahedral sites are high spin (weak CF).

For $x = 0.25$, there are three tetrahedral ions and one octahedral Co^{2+} ion, and one tetrahedral and seven octahedral Fe^{3+} ions in the adopted 28-atom unit cell. The spins at tetrahedral sites are antiparallel to those at octahedral sites in the spinel structure. The favourite electronic configuration is calculated to be as follows. Each tetrahedral Co^{2+} ion contains three unpaired electrons at the t_{2g} levels, while the octahedral Co^{2+} ion contains one unpaired electron at t_{2g} and two unpaired electrons at e_g levels, respectively. Each tetrahedral or octahedral Fe^{3+} ion contains five unpaired electrons at e_g and t_{2g} levels, as schematically shown in figure 4, resulting in a final spin configuration of $6\mu_B$ per CoFe_2O_4 unit. The same explanation can be applied to the spinel with $x = 0.5$ and $x = 0.75$, exhibiting a final spin configuration of $5\mu_B$ and $4\mu_B$ per CoFe_2O_4 unit, respectively. In [49], the authors gave only the average magnetic moment of Co and Fe at the corresponding sites, which are $-3.08\mu_B$ for the A site and $3.21\mu_B$ for the B site. Actually, our calculated magnetic moment at both A and B sites depends on the type of cations strongly, although the calculated average magnetic moments

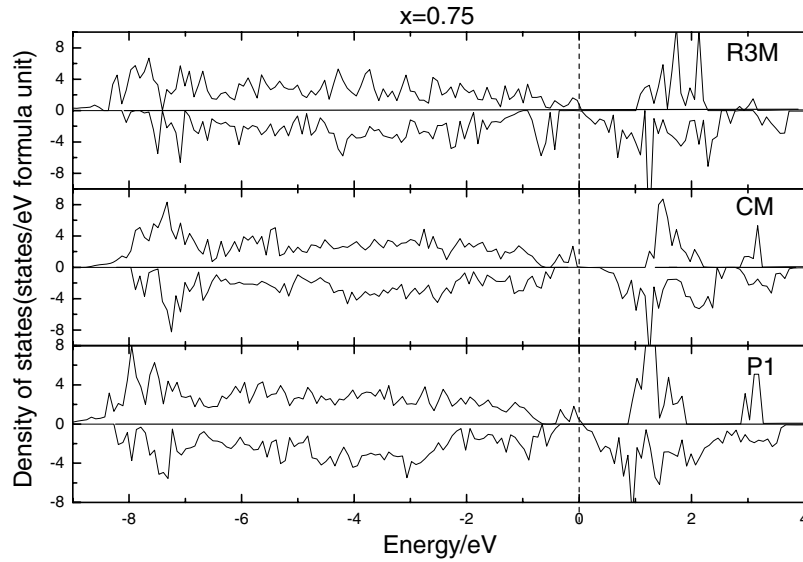


Figure 5. TDOS of $(\text{Co}_{1-x}\text{Fe}_x)_{\text{Tet}}(\text{Co}_x\text{Fe}_{2-x})_{\text{Oct}}\text{O}_4$ at $x = 0.75$ considered spinel structure. The minority DOS is set to negative, while the majority part is set to positive. VBM is set to 0.

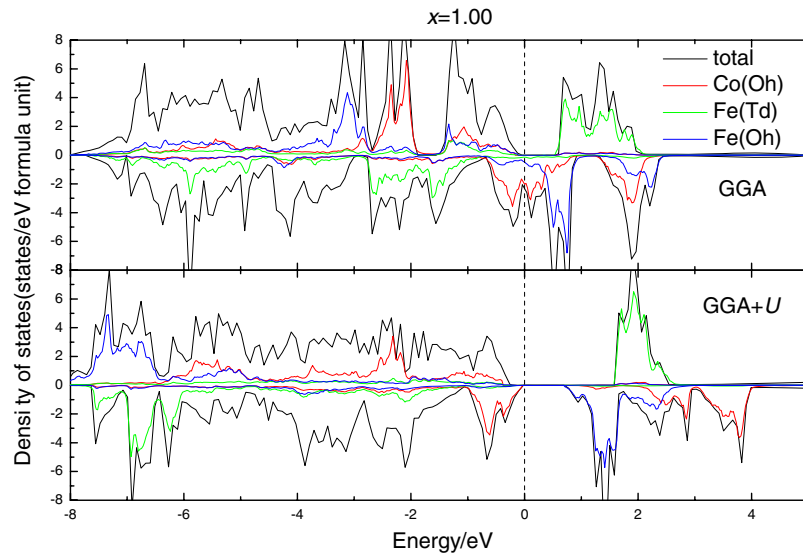


Figure 6. The atom-projected DOS and TDOS of CoFe_2O_4 with the inverse spinel structure. The minority DOS is set to negative, while the majority part is set to positive. VBM is set to 0.

for A and B sites are consistent with the experimental values (-3.19 and $3.36\mu_B$ versus -3.08 and $3.21\mu_B$). There is no remarkable difference between the two studied structures (*CM* and *R3M* of $x = 0.25$) on their magnetic moment, but clearly different on the electronic structure. The system of $0.25(\text{CM})$ is insulating with a band gap of 0.08 eV, while $0.25(\text{R3M})$ is a half-metal. For $0.25(\text{R3M})$, a sharp peak in the vicinity of Fermi energy in the minority spins implies the configuration is unstable, in line with its relatively higher energy. A similar situation is found in the spinels (*C2M*, *CM* and *P-1*) at $x = 0.50$ and (*CM*, *P1* and *R3M*) at $x = 0.75$. In the $x = 0.50$ case, it shows that $0.50(\text{C2M})$ and $0.50(\text{CM})$ are insulating with band gaps of 0.16 eV and 0.24 eV, respectively, while the $0.50(\text{P-1})$ structure is a half-metal. In the case of $x = 0.75$, it shows that the $0.75(\text{CM})$ structure is insulating with a

band gap of 0.30 eV, while both $0.75(\text{P1})$ and $0.75(\text{R3M})$ spinel structures are half-metallic as shown in figure 5. It is worth noting that the systems are always insulating for the configurations of the lowest energy for a given x .

In the case of ideal inverse spinel at $x = 1.0$, the PDOS (cf figure 6) indicates that Co is in the $2+$ state, and Fe is in its $3+$ state at both tetrahedral and octahedral sites. Since the spin in the tetrahedral sites is always antiparallel to that in the octahedral sites, the magnetic moment of Fe^{3+} are cancelled out, leaving the only net contribution from Co^{2+} , which gives a final magnetic moment of $3\mu_B$ per CoFe_2O_4 formula. Figure 6 compares the DOS of inverse cobalt ferrite given by GGA and GGA + U calculations. It shows that cobalt ferrite in the inverse spinel structure is a half-metal in GGA calculation and becomes insulating with a band gap of 0.72 eV when GGA + U

is applied. The result given by GGA + U calculation is in reasonable agreement with the earlier reported self-interaction corrected DFT [34] value of 0.8 eV, LDA + U [32] value of 0.63 eV and GGA + U [33] value of 0.52 eV. To the best of our knowledge no experimental reports of the band gap of CoFe_2O_4 have been available. However, conductivity measurements indicate an electronic gap in the region of 0.5–0.6 eV for stoichiometric CoFe_2O_4 [48].

4. Conclusions

In this study, the CoFe_2O_4 spinel was systematically investigated by GGA and GGA+ U calculations. Our results show that CoFe_2O_4 energetically favours inverse spinel ($x = 1$) and both Fe and Co always prefer high spin configuration, no matter whether in octahedral or tetrahedral sites in the partial inverse spinels. As x increases, the total magnetic moment of CoFe_2O_4 decreases. The lattice parameter of the spinel increases slightly with increasing inversion parameter x . The Co ions in the partial inverse spinel favour being far away from each other, allowing a reasonable study of the system with relatively small unit cells.

Acknowledgments

The authors acknowledge the computer time at the High Performance Grid Computer Center of South China University of Technology (SCUTGrid). This work was supported by the Natural Science Foundation of China (Grant Nos U0734001 and 50874050), the Natural Science Foundation of Guangdong Province (Grant No 8151064101000084), Guangdong Provincial Science and Technology Programme (Grant No 2008B010600005), the Fundamental Research Funds for the Central Universities, SCUT (Grant Nos 2009ZZ0025, 2009ZM029 and 2009ZM0247).

References

- [1] Cox P A 1992 *Transition Metal Oxides* (Oxford: Oxford University Press)
- [2] Hill R J, Craig J R and Gibbs G V 1979 *Phys. Chem. Miner.* **4** 317
- [3] Sun S H, Zeng H and Robinson D B 2004 *J. Am. Chem. Soc.* **126** 273
- [4] Gabal M A and Ata-Allah S S 2004 *Mater. Chem. Phys.* **85** 104
- [5] Brabers V A M 1997 *Handbook of Magnetic Materials* vol 8 (Amsterdam: Elsevier Science)
- [6] Chen Y, Snyder J E, Schwichtenberg C R, Dennis K W, McCallum R W and Jiles D C 1999 *IEEE Trans. Magn.* **35** 3652
- [7] Lisfi A and Williams C M 2003 *J. Appl. Phys.* **93** 8143
- [8] Jeng H T and Guo G Y 2002 *J. Magn. Magn. Mater.* **239** 88
- [9] Slonczewski J C 1958 *Phys. Rev.* **110** 1341
- [10] Chinnasamy C N, Jeyadevan B, Shinoda K, Tohji K, Djayaprawira D J, Takahashi M, Justin Joseyphus R and Narayanasamy A 2003 *Appl. Phys. Lett.* **83** 2862
- [11] Chinnasamy C N, Jeyadevan B, Perales-Perez O, Shinoda K, Tohji K and Kasuya A 2002 *IEEE Trans. Magn.* **38** 2640
- [12] Ammar S, Helfen A, Jouini N, Fiévet F, Rosenman I, Villain F, Molinié P and Danot M 2001 *J. Mater. Chem.* **11** 186
- [13] Giri A K, Kirkpatrick E M, Moongkhamklang P, Majetich S A and Harris V G 2002 *Appl. Phys. Lett.* **80** 2341
- [14] Zheng H, Wang J, Lofland S E, Ma Z, Mohaddes-Ardabili L, Zhao T, Salamanca-Riba L, Shinde S R, Ogale S B, Bai F, Viehland D, Jia Y, Schlom D G, Wuttig M, Roytburd A and Ramesh R 2004 *Science* **303** 661
- [15] Chopdekar R V and Suzuki Y 2006 *Appl. Phys. Lett.* **89** 182506
- [16] Zheng H, Straub F, Zhan Q, Yang P-L, Hsieh W-K, Zavaliche F, Chu Y-H, Dahmen U and Ramesh R 2006 *Adv. Mater.* **18** 2747
- [17] Bhamé S D and Joy P A 2006 *J. Appl. Phys.* **100** 113911
- [18] Gul I H, Abbasi A Z, Amin F, Anis-ur-Rehman M and Maqsood A 2007 *J. Magn. Magn. Mater.* **311** 494
- [19] Bersuker I B 1996 *Electronic Structure and Properties of Transition Metal Compounds: Introduction to the Theory* (New York: Wiley)
- [20] Burns R 1993 *Mineralogical Applications of Crystal Field Theory* (Cambridge: Cambridge University Press) vol 5
- [21] Borg R J and Dienes G J 1992 *The physical chemistry of solids* (Academic: San Diego, CA)
- [22] Na J G, Lee T D and Park S J 1993 *J. Mater. Sci.* **12** 961
- [23] Van M Meerssche and Feneau-Dupont J 1984 *Introduction à la cristallographie et à la chimie structurale* (Leuven, Belgium: Peeters)
- [24] Ferreira T A S, Waerenborgh J C, Mendonça M H R M, Nunes M R and Costa F M 2003 *Solid State Sci.* **5** 383
- [25] Sawatzky G A, Van Der Woude F and Morrish A H 1969 *Phys. Rev.* **187** 747
- [26] Sawatzky G A, Van Der Woude F and Morrish A H 1968 *J. Appl. Phys.* **39** 1204
- [27] Murray P J and Linnett J W 1976 *J. Phys. Chem. Solids* **37** 1041
- [28] Murray P J and Linnett J W 1976 *J. Phys. Chem. Solids* **37** 619
- [29] Uzunova E L, Mitov I G and Klissurski D G 1997 *Bull. Chem. Soc. Japan* **70** 1985
- [30] Waseda Y, Shinoda K and Sugiyama K 1995 *Z. Naturforsch.* **50a** 1199
- [31] Pénicaud M, Siberchicot B, Sommers C B and Kübler J 1992 *J. Magn. Magn. Mater.* **103** 212
- [32] Antonov V N, Harmon B N and Yaresko A N 2003 *Phys. Rev. B* **67** 024417
- [33] Walsh A, Wei S-H, Yan Y, Al-Jassim M M and Turner J A 2007 *Phys. Rev. B* **76** 165119
- [34] Szotek Z, Temmerman W M, Ködderitzsch D, Svane A, Petit L and Winter H 2006 *Phys. Rev. B* **74** 174431
- [35] Wyckoff R 1964 *Crystal Structures* 2nd edn (New York: Wiley-Interscience)
- [36] Gracia L, Beltran A, Andrés J, Franco R and Recio J M 2002 *Phys. Rev. B* **66** 224114
- [37] Kresse G and Furthmüller J 1996 *Phys. Rev. B* **54** 11169
- [38] Kresse G and Furthmüller J 1996 *Comput. Mater. Sci.* **6** 15
- [39] Perdew J P, Burke K and Ernzerhof M 1996 *Phys. Rev. Lett.* **77** 3865
- [40] Blöchl P E 1994 *Phys. Rev. B* **50** 17953
- [41] Kresse G and Joubert D 1999 *Phys. Rev. B* **59** 1758
- [42] Liechtenstein A I, Anisimov V I and Zaanen J 1995 *Phys. Rev. B* **52** R5467
- [43] Dudarev S L, Botton G A, Savrasov S Y, Humphreys C J and Sutton A P 1998 *Phys. Rev. B* **57** 1505
- [44] Solov'yev I V, Dederichs P H and Anisimov V I 1994 *Phys. Rev. B* **50** 16861
- [45] Hemeda O M and Barakat M M 2001 *J. Magn. Magn. Mater.* **223** 127
- [46] Shannon R D 1976 *Acta Crystallogr. A* **32** 751
- [47] Nlebedim I C, Ranvah N, Williams P I, Melikhov Y, Snyder J E, Moses A J and Jiles D C 2010 *J. Magn. Magn. Mater.* **322** 1929
- [48] Jonker G H 1959 *J. Phys. Chem. Solids* **9** 165
- [49] Liu Chao, Zou Bingsuo, Rondinone Adam J and Zhang Z John 2000 *J. Am. Chem. Soc.* **122** 6263